

Novel method of generating water-in-oil(W/O) droplets in a microchannel with grooved walls

Jihoon Kim,¹ Doyoung Byun,^{1,a)} and Jongin Hong²

¹*Department of Aerospace Information Engineering, Konkuk University, Seoul 143-701, South Korea*

²*Department of Chemistry, Chung-Ang University, Seoul 156-756, South Korea*

(Received 12 October 2010; accepted 17 February 2011; published online 15 March 2011)

We present a novel method of generating and retrieving droplets stored in microfluidic grooves or cavity structures. First we designed and fabricated polydimethylsiloxane microchannels with grooves on the walls and then produced a two-phase flow of oil and aqueous phases to form aqueous phase droplets in an oil state. We propose the following three mechanisms of droplet generation: the contact line on the groove wall continues moving along the wall and descends to the bottom of the cavity, confining the aqueous phase in the cavity; once the interface between the oil and aqueous phases moves into the cavity, the interface contacts the top of the neighboring groove; and a spherical droplet forms at the corner in the cavity due to surface tension. The viscosity of the oil phase and the surface tension of the interface determine whether a droplet can be generated. Then, we could adjust the velocity of the interface and the aspect ratio of the cavity to achieve the optimal conditions for generating the single droplet. We observed that the largest droplet is stably generated without a daughter droplet at typical values of free-stream velocity (10 $\mu\text{l}/\text{min}$) and groove pitch 110 μm for all three cases with different oil phases (20, 50, and 84 cP). This technique is expected to serve as a platform for droplet-based reaction systems, particularly with regard to monitoring cell behavior, *in vitro* expression, and possibly even micropolymerase chain reaction chambers.

© 2011 American Institute of Physics. [doi:10.1063/1.3567102]

I. INTRODUCTION

During the past decade, a wealth of research has been dedicated to elucidating the flow characteristics in microchannels and nanochannels for microfluidic systems.¹ These devices can generate, pump, and transport minute quantities of fluids, such as microliter or picoliter droplets.^{1,2} Microfluidic devices for droplet formation, merging, and transporting have been developed as fundamental platforms for high-throughput experimentation. Droplet-controlled microfluidic systems are beneficial for fundamental research fields, such as chemistry analysis, as well as various forms of applied technology in biology and medical devices, such as lab-on-a-chip technology.²⁻⁵ Droplets may be used for applications involving incubation, sorting, storage of biological or chemical materials in various areas, and droplet-based reactions such as micropolymerase chain reactions.^{4,6} Droplet generation in an immiscible state has been diversely studied for liquid-liquid flows, such as oil-in-water and water-in-oil flows. To date, researchers have largely focused on many kinds of techniques, one example involving geometrical shapes of T- or Y-junctions and another based on a flow-focusing method.^{2,7-11} Both methods benefit from the ease of control provided by droplet-based systems. Without hydrodynamic techniques, alternative methods are attracted. The electrowetting on dielectrics (EWOD) technique is generated droplet moving, merg-

^{a)} Author to whom correspondence should be addressed. Electronic mail: dybyun@konkuk.ac.kr. Tel.: +82 (2) 450-4195. FAX: +82 (2) 444-6670.

ing, and separating by electrode array.^{12–14} The surface acoustic wave are manipulated a droplet which is located inside lab-on-a-chip.^{15–17} One of the vibrators, an ultrasonic, can generate typical size of droplets.^{18,19} However, the task of rapidly generating droplets in cell structures is not easy.

Many researchers have investigated apparent fluid slips due to hydrophobic surfaces in microscale and nanoscale flows and studied slip length in the microchannels.^{20–29} Other studies also investigated nanoscale microchannels.^{30,31} It has been suggested that nanobubbles entrapped in the valleys of rough, hydrophobic surfaces affect the slippage of liquid flows in microchannels.³² The complex behavior of the fluid-solid interaction involves the physical and chemical properties of the hydrophobic surfaces, particularly the wettability of the solid, the presence of impurities and dissolved gases, as well as the shear rate, pressure, surface charge, and surface roughness. Due to these complex interactions, the observed slip lengths range from nanometers to micrometers that directly measure the slip length in a superhydrophobic microchannel with grooved walls.²⁰ Since the appearance of the Wenzel³³ and Cassie–Baxter³⁴ models 60 years ago, many groups have investigated how the size and shape of microstructures affect the hydrophilicity and hydrophobicity of different materials.^{35–38} The Wenzel state refers to a liquid droplet that completely wets the asperities of a rough surface; the Cassie–Baxter state, on the other hand, refers to a liquid droplet which is suspended on top of a rough surface and which leaves air pockets inside the rough structures. It has been noted that liquid droplets on superhydrophobic surfaces can transition from the higher energy Cassie–Baxter state to the lower energy Wenzel state if they overcome the energy barrier between the two states by filling the asperities with liquid and forming a more stable homogeneous interface due to geometric effects or external pressure.

In this paper, we investigate the flow characteristics of two immiscible liquids in a grooved microchannel with respect to the generation of liquid droplets. Even though the T- or Y-junction approaches and the flow-focusing methods provide ease of generation and control of uniform monodisperse droplets, the task of rapidly generating droplets in cell structures is not easy. Therefore, we suggest a novel method of generating, storing, and retrieving droplets in the cavity structure between grooves and investigate how the geometry of the grooves and the physical properties of the fluids, such as viscosity, affect the generation of droplets.

II. EXPERIMENTAL METHOD

A. Fabrication

Silicon groove patterns, which serve as a mold during the polydimethylsiloxane (PDMS) molding process and generate anisotropic groove surfaces, are fabricated, as shown in Fig. 1, with a process of lithography and deep reactive ion etching. The details of the fabrication can be found in a previous work.²⁰ The PDMS microchannel with grooves is bonded to a PDMS flat surface. On both side walls, grooved structures are created to allow for groove characteristics, and smooth PDMS surfaces are retained on the top and at the bottom. A soft contact method is used for the PDMS-PDMS bonding method. The PDMS is mixed with a solvent (Sylgard 184 A & B, Dow Corning, Inc.) at a volume ratio of 10:1, poured on a patterned substrate, cured for 10–15 min at 95 °C, and then peeled off from the substrate. Another sample of liquid PDMS is poured on a nonpatterned flat substrate and cured for 20–30 min at 65 °C. The PDMS microchannel is then bonded to the flat PDMS surface. After being peeled off from the mold master, the patterned PDMS is bonded with the nonpatterned flat PDMS surface through the application of pressure. After both parts have been bonded, the device is recured for 4 h at 65 °C.

Table I shows the dimensions of the grooved structures on the microchannel walls, where the droplets form as a result of the interaction of the aqueous phase and oil flows. In our experiment, we fixed the microchannel length at 30 mm and the width at 200 μm . The groove had a width of 15 μm , a depth of 20 μm , a height of 45 μm , and a varied pitch of 80–140 μm .

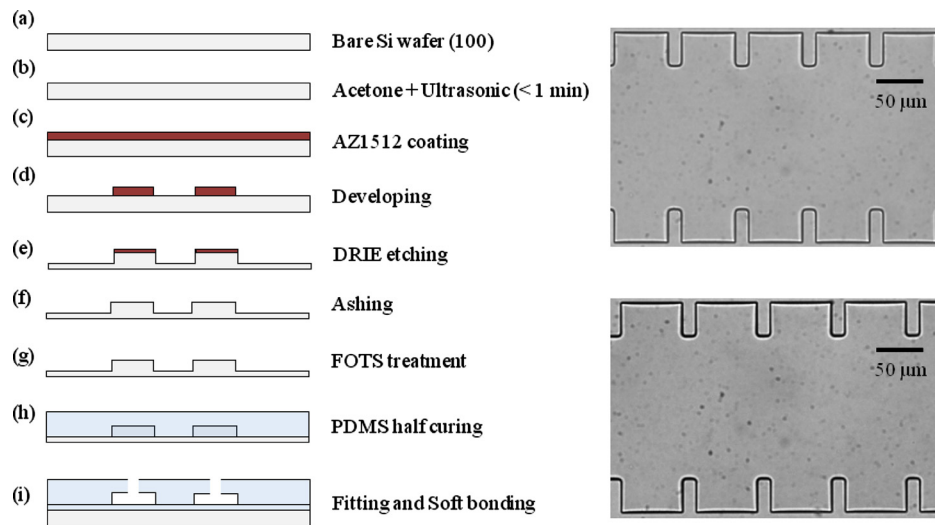


FIG. 1. Fabrication process of groove patterns in a microchannel (left) and top-view of groove patterns (right).

B. Experimental setup

Figure 2 shows a schematic and a photo of the experimental setup. Included are an inverted microscope (Nikon Eclipse TE2000, Nikon Co., Ltd.) and a 1380×1040 resolution charge-coupled device (CCD) camera (Sensicam QE, PCO Co., Ltd.) for acquiring images. A 200 magnification objective lens, whose numerical aperture is 1.515, is used to capture the flow field near the wall in the microchannel. Simultaneously, the aqueous phase that is used for the wetting transition experiments consists of a 78:22 (volume ratio) mixture of water and glycerin. For the droplet generation experiment, aqueous solution (e.g., a mixture of water and glycerin) and oil are used. Due to the difference of reflective index between aqueous solution and oil, liquid meniscus is finely visualized at interested section. A precision syringe pump (11 plus, Harvard Co., Ltd.) is used to deliver liquids at flow rates ranging from 5 to 15 $\mu\text{l}/\text{min}$.

To supply two liquids with an interface between them, we first supply an aqueous phase to a Teflon tube via a syringe pump. Once the aqueous phase fills the whole microchannel and the cavities between the grooves, the oil phase is supplied to form an interface. The time required for complete wetting in the cavities varies in relation to the groove pitches and flow rates. The wetting transition phenomena occur around 3–6 min later. From the opposite side of the microchannel, we then connect another syringe pump and supply immiscible oil.

III. RESULT AND DISCUSSION

Liquid on groove surfaces can transition from the higher energy Cassie–Baxter state to the lower energy Wenzel state; the energy barrier between the two states is overcome when the liquid fills the asperities and forms a more stable homogeneous interface.³⁵ The Cassie–Baxter state is strongly related to both the chemical composition and the geometry of the surface. There has been a significant amount of research on stabilization of the composite interface and formulation of the

TABLE I. Dimensions of groove structure in the microchannel.

The range of pitch: 80–140 μm			
Depth (μm)		20	
Width (μm)		15	
Height (μm)		45	
Flow rate ($\mu\text{l}/\text{min}$)	5	10	15

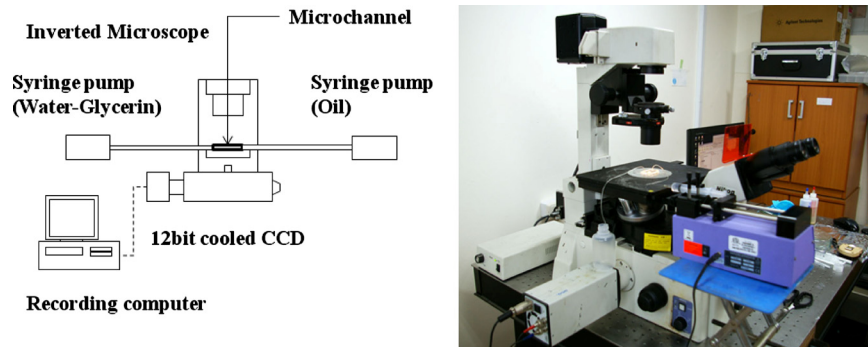


FIG. 2. A schematic and a photo of experimental setup.

transition criteria for steady liquid droplets on the surface. The stability of the composite solid-air-liquid interface is very important for maintaining the groove in the microchannel. In a previous study, we observed the wetting transition in a microchannel with grooved structures.²⁰ Parametric studies were carried out by varying the width (5 and 14 μm), pitch (12.5–45 μm and 35–126 μm for two width structures, respectively), and flow rate (2.4–9.6 $\mu\text{l/min}$). For the range of flow rates considered, there was no critical effect of the flow rate on the wetting transition or the transition time when it occurs. For both microchannels with 5 and 14 μm wide grooves, a transition occurred when the pitch-to-width ratio was around 8 or 9. When the pitch between the grooves in the microchannel increased, the pressure difference between the liquid and gas phases was attributed to the penetration of the meniscus into the cavity.

An aqueous phase and oils are used for the droplet generation experiment. Figure 3 presents a schematic of our proof of concept in a grooved microchannel where the wetting transition phenomenon is exploiting. Before the droplet generation, the whole surface of the microchannel must be wetted. As noted with regard to a wetting transition experiment described in a previous

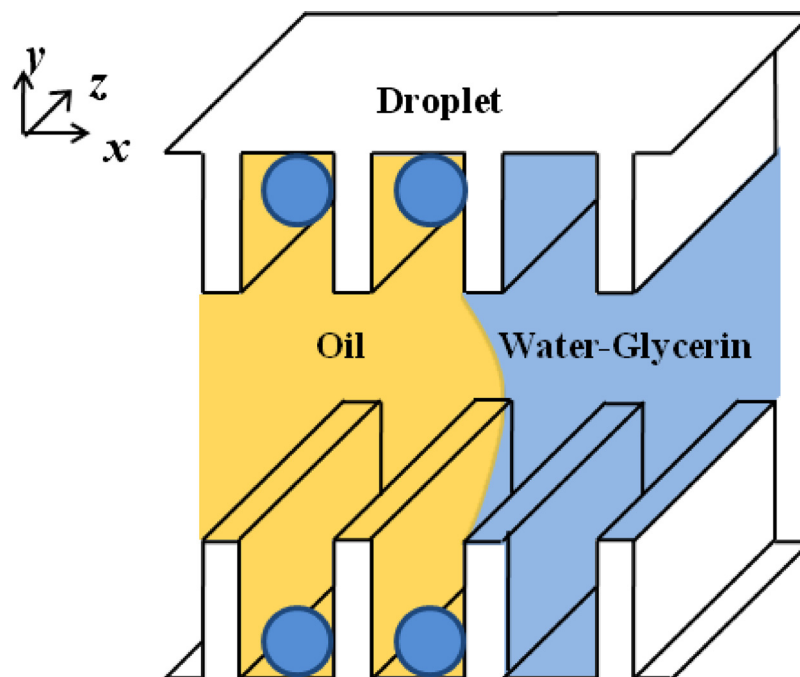


FIG. 3. A schematic of droplet generation in the groove microchannel.

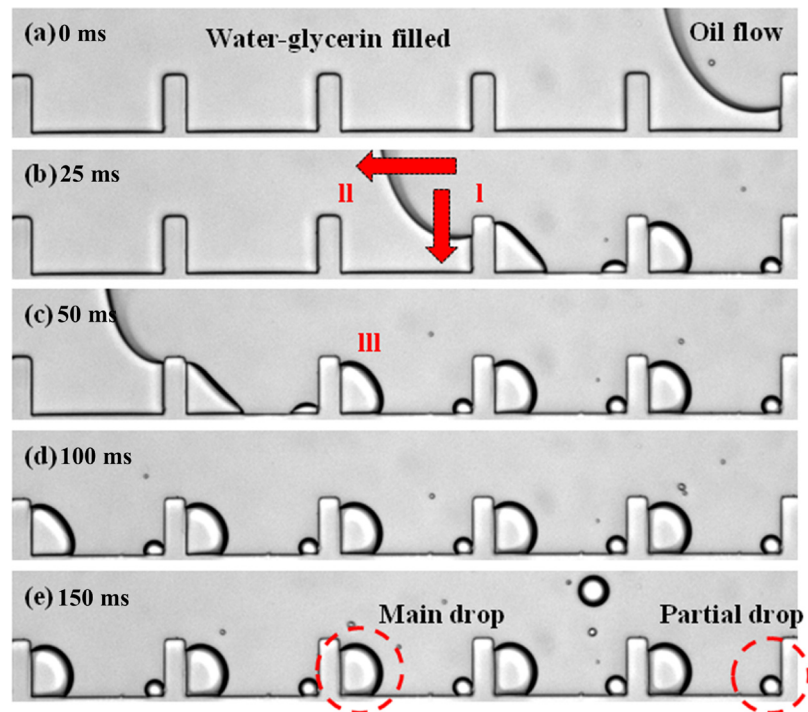


FIG. 4. Sequential images of meniscus movement and mechanism of droplet generation.

work,²⁰ the wall is comprised of laterally alternating grooves and cavities. If the pitch between the microgrooves is small enough and the surfaces are hydrophobic, the liquid does not wet or enter cavities. When the pitch is large enough, the liquid fully wets the inside of the grooves with an appropriate flow rate. The factors of groove size, including the pitch and height, which are necessary for determining the wetting, depend on the liquid-solid interfacial chemistry, the interfacial tension between liquid and solid, and the pressure difference between the gas and liquid phases. If the spacing between grooves is large enough, the liquid fully wets the grooves.

The cavities on the side walls are presumed to facilitate the formation and storage of microdroplets if we use two immiscible fluids, such as water and oil. The mechanism underlying our approach can be briefly summarized as follows. First, a microchannel is filled with sequentially flowing aqueous and oil phases; the oil replaces the aqueous phase except for a small portion of the aqueous phase inside the grooves; finally, because of the equilibration of interfacial tension, stationary aqueous phase droplets are formed in a continuous phase of oil. To investigate the properties of oil, we evaluated four kinds of oil: commercial olive oil, two silicone oils (DC 200, Sigma-Aldrich Co., Ltd.), and Fluorinert FC-3283 (3M Co., Ltd.). The oils have very different viscosities (namely, 84, 50, 20, and 1.4 cP, respectively).

Figure 4 shows the sequential images of the meniscus movement of the olive oil (84 cP viscosity) and aqueous phases when the groove pitch is 120 μm and the flow rate is 10 $\mu\text{l}/\text{min}$. The figure depicts the generation of two kinds of droplets: a main drop in the left corner of the cavity and a partially formed drop, called a daughter drop, in the right corner. When the interface of the oil-aqueous phase moves and penetrates a cavity on the vertical or horizontal wall, the oil replaces the aqueous phase in a recirculating zone of the cavity. The insets display the sequential images of droplet generation at a flow rate of 10 $\mu\text{l}/\text{min}$ with a pitch of 120 μm . When the interface of the two immiscible liquids moves across the cavity between the two neighboring grooves, the oil phase may replace the aqueous phase in the cavity, isolating the aqueous phase in a corner or both corners of the cavity and forming a droplet. The isolated aqueous phase volume

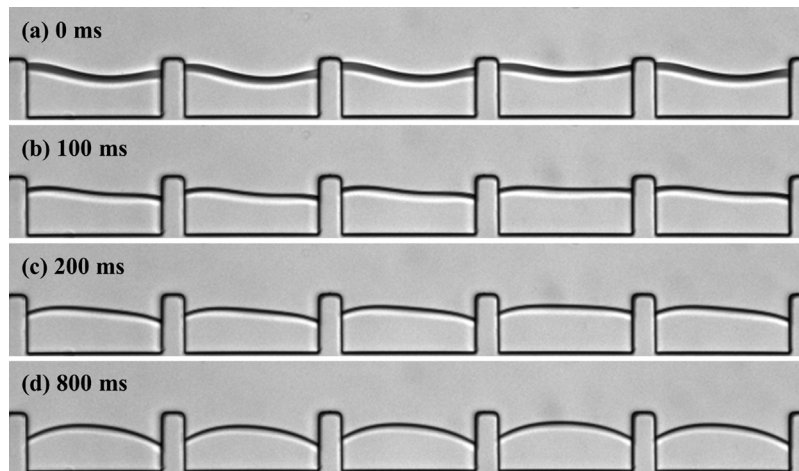


FIG. 5. Sequential images of two immiscible liquids of aqueous phase and low viscosity oil phase (FC-3283, 3M Co., Ltd.).

directly affects the droplet size, which is determined by the speed of the interface, the geometry of the grooves, and the physical properties of fluids, such as viscosity and surface tension.

Note that there are three distinct mechanisms of droplet generation. With regard to the first, the contact line on the groove wall should continue moving along the wall and descend to the bottom of the cavity, confining the aqueous phase in the cavity; this phenomenon is related to the viscous force and, consequently, to the viscosity of the oil phase. When the viscosity of the oil (FC-3283, 3M Co., Ltd.) is low and similar to that of the aqueous phase, as shown in Fig. 5, the oil phase cannot penetrate the cavity and, as a result, it cannot isolate the aqueous phase or form any droplets in the cavity. Figure 5 shows the sequential images of interface movements between two immiscible liquids of the aqueous phase and FC-3283 (3M Co., Ltd.), the viscosity of which is only 1.4 cP. Even though the groove pitch ($120\ \mu\text{m}$) and the flow rate ($10\ \mu\text{l}/\text{min}$) correspond with the results reported in Fig. 4, no droplet is generated and only the aqueous phase fills the cavity. This tendency is mainly due to the low viscosity of the oil, which may prevent the meniscus from attaching itself to the wall, penetrating along the cavity, and pushing the aqueous phase into the left corner of the cavity. One report that highlights the importance of the relative viscosity between the discrete and continuous phases has confirmed that the selection of a more viscous continuous phase facilitates the formation of droplets for the well-known T- or Y-junction method and the flow-focusing method.⁵ Once the interface between the oil and aqueous phases moves into a cavity and across a groove, as shown in Fig. 4, the interface should make contact with the top of the neighboring groove, isolating the aqueous phase in the left corner. This contact and the isolation of the aqueous phase represent the second mechanism; they also determine the size of each droplet. In the third mechanism, a spherical droplet forms at the corner due to surface tension.

Similar to this study, the droplets or rings could be generated by contact-line precipitation, hydrophobic patches, actuated valves, and acoustic waves.^{39–42} However, these technologies require the external actuation to generate droplets such as valve operation or power for the acoustic wave. Moreover, in our grooved microchannel, the droplets could be passively generated and stored based on the optimized geometry and fluidic condition.

As shown in Fig. 6, we can categorize four modes of droplet generation in the cavities: a filling cavity mode (no droplet generation), a main droplet mode, a main droplet and daughter droplet mode, and a trapping mode. The filling cavity mode represents the case where there is no droplet generation and, as shown in Fig. 6, the aqueous phase just fills the cavity. Usually this mode occurs for low viscosity oil. As the viscosity of the oil increases, we can observe the other three modes of droplet generation. When the interface between the oil and aqueous phases moves

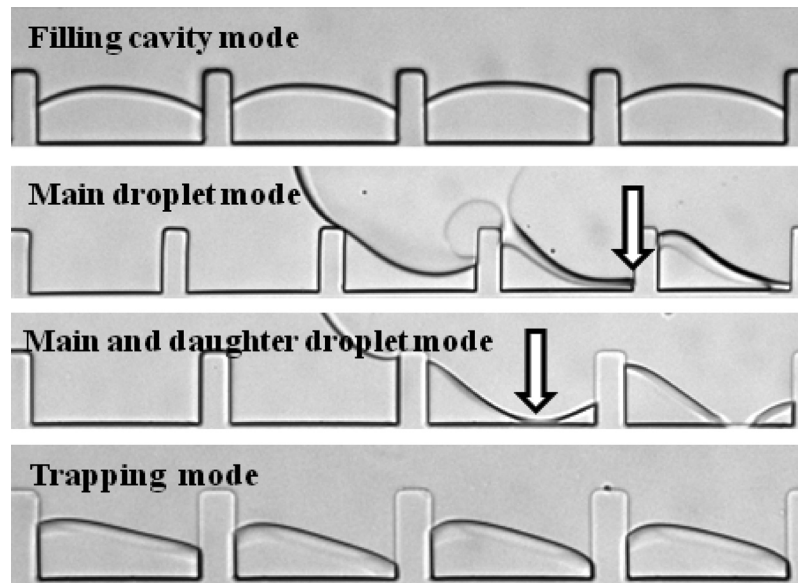


FIG. 6. Various types of droplet generation mode: (a) filling cavity mode (no droplet generation), (b) main droplet mode, (c) main and daughter droplet mode, and (d) trapping mode (droplet generation due to surface tension).

into a cavity, the interface reaches a point on the bottom, which is referred to as an attachment point (AP). When the interface moves right or left, the aqueous phase is trapped in the grooves. If the interface moves down along the vertical wall in the cavity and touches the right corner, as shown in Fig. 6(b), a large single droplet can be formed; this phenomenon is referred to as the main droplet mode. When the AP is located at the middle of the bottom wall, the aqueous phase exists in both the right and left corners and, as shown in Fig. 6(c), forms the main and daughter droplets. The size of the daughter droplet depends on the location of the AP. Under some conditions, the AP does not make contact with the bottom when the interface between the aqueous phase and oil is in contact with the top of the neighboring groove; this behavior isolates the aqueous phase in the cavity and creates the largest droplet. Figure 6(d) shows this trapping mode. There are many parameters which affect the AP, such as the viscosity, the wettability of the groove wall, the interfacial tension, flow rate, and the aspect ratio. The interface has to be moved downward into the cavity to generate the droplet.

As noted earlier, in order to investigate the effects of viscosity, we used four kinds of oils with different viscosities. We also measured the surface tension between the aqueous phase and the oils by using a spinning drop tensiometer (SITE 100, KRUSS Co., Ltd.). The measured interfacial tensions are 41.8, 14.0, 15.6, and 15.7 mN/m for the interfaces between aqueous phases and Fluorinert FC-3283 (1.4 cP), silicone oil (20 cP), silicone oil (50 cP), and commercial olive oil (84 cP), respectively.

Figure 7 shows how the groove pitch and the flow rate affect the diameter of droplets isolated in the cavities for the three oil phase fluids with different viscosities. The sequential images in Fig. 7 depict the main droplet generation process without any partial droplets for all three cases. These experiments confirm that optimal conditions of the pitch and flow rate exist for the stable generation of large droplets. The pitch of the grooves and the flow rate (velocity) affect the size of the recirculating zone in the cavities and, hence, the droplet diameter. In our experiments, the diameter of the isolated droplets ranges from around 10 to 50 μm , depending on the oil phase flow rate and the pitch of the groove. For every case, as shown in Fig. 7, we can observe the stable generation of the largest droplets in the cavities when the pitch of the grooves is 110 μm and the flow rate is 10 $\mu\text{l}/\text{min}$. When the pitch is higher or lower than 110 μm at a flow rate of 10 $\mu\text{l}/\text{min}$, the droplet size decreases and a daughter droplet is generated. At a pitch of 110 μm , the droplet size decreases or a daughter droplet is generated when the flow rate is larger or smaller than

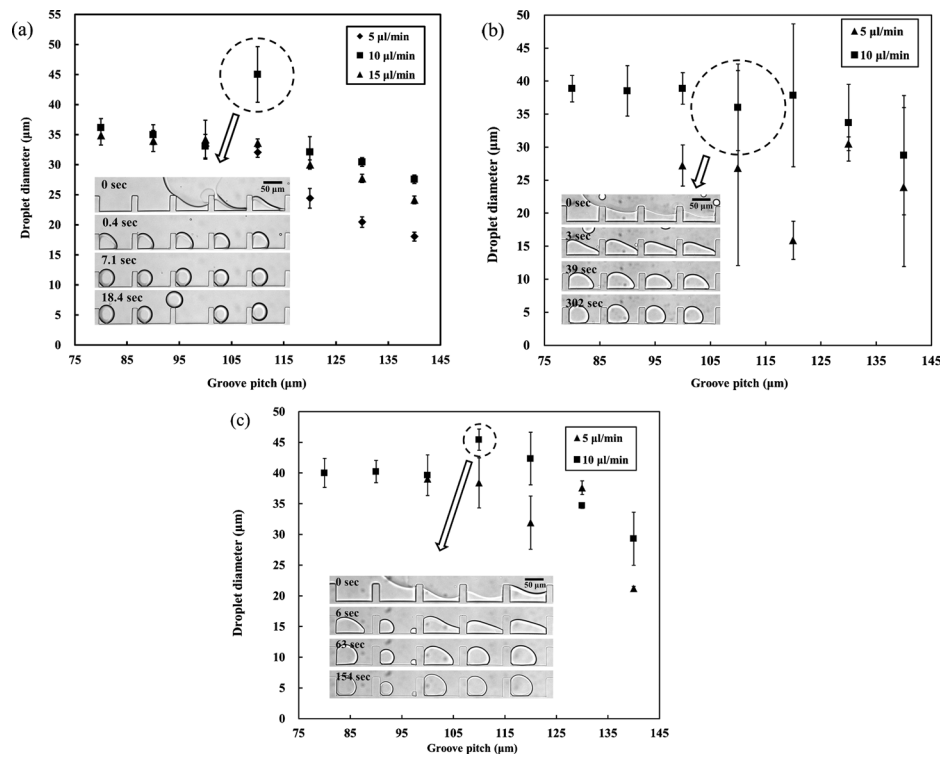


FIG. 7. Effects of groove pitch and flow rate on droplet diameter: (a) aqueous phase and olive oil (84 cP), (b) aqueous phase and silicone oil (50 cP), and (c) aqueous phase and silicone oil (20 cP).

10 $\mu\text{l}/\text{min}$. This behavior means that droplets can be optimally formed when the flow rate and the pitch size are well matched. Interestingly, under the optimal conditions, uniform droplets can be generated without daughter droplets in the cavities. Occasionally, as shown in Fig. 7(c), there is a partial droplet in one of the cavities even under the optimal conditions. As we mentioned, the movement of the contact line along the groove wall determines the mode of forming droplets. If there are defects on the PDMS groove wall such as surface roughness uniformity and wettability, the contact line moves unstably at any local cavity in the grooved microchannel. We counted the number of partial droplet formation under the optimal condition. For the case of 110 μm pitch, the probability of the partial droplet formation is around 4%. It means that four partial droplets statistically appear in 100 cavities.

Figure 8 describes the pattern of droplet generation according to the flow rate when the pitch is 110 μm and the flow rate is varied from 5 to 15 $\mu\text{l}/\text{min}$. If the flow rate is high (15 $\mu\text{l}/\text{min}$),

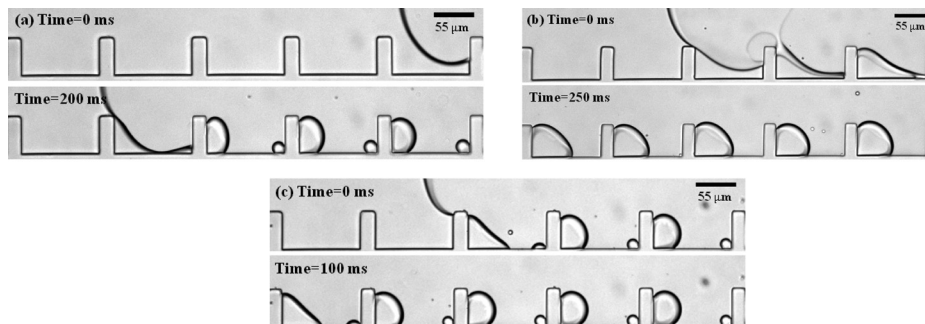


FIG. 8. Sequential images of droplet generation according to flow rate: (a) 5 $\mu\text{l}/\text{min}$, (b) 10 $\mu\text{l}/\text{min}$, and (c) 15 $\mu\text{l}/\text{min}$.

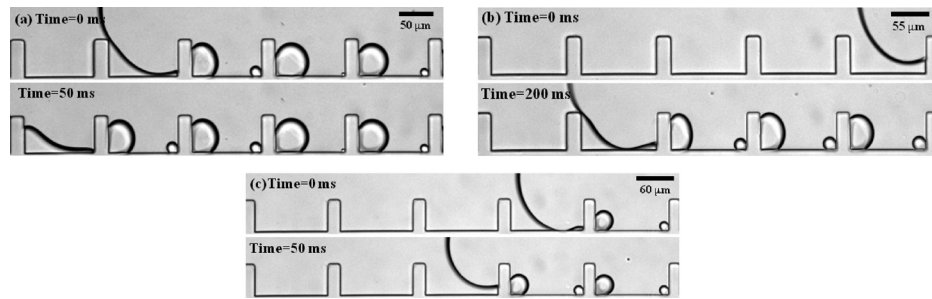


FIG. 9. Sequential images of droplet generation according to pitch with flow rate of $5 \mu\text{l}/\text{min}$: (a) $100 \mu\text{m}$, (b) $110 \mu\text{m}$, and (c) $120 \mu\text{m}$.

the interface between the two immiscible liquid phases passes too quickly through the cavity to generate stable droplets. The interface contacts the middle of the bottom surface in the cavity, which means that the AP exists in this location. Therefore, daughter droplets can be generated in the right corner due to the confined aqueous phase. Similarly, when the flow rate is slower ($5 \mu\text{l}/\text{min}$), as shown in Fig. 8(a), daughter droplets are generated in the right corner of the cavities because the AP is located in the middle of the bottom surface. Figure 8(a) shows that when the interface makes contact with the top surface of the left groove, the interface also makes contact with the bottom wall due to a low flow rate and does so before the interface contact line on the vertical wall moves down to the bottom wall. Therefore, daughter droplets can be generated due to the isolation of the aqueous phase in the right corner. Figure 8(b) is a good example of optimal droplet generation due to simultaneous contact of the interface on the top of the left groove and on the right corner of the cavity. Accordingly, the motion of the two-phase interface on the wall is important for determining the formation of daughter droplets. If the two-phase interface makes contacts earlier or later, the main droplet is formed in the forward corner of the cavity and the daughter droplet is formed in the backward corner of the cavity. Note also that the contact-line movement on the wall is strongly related to the difference of viscosity and the surface tension between the oil and aqueous phases.

Figure 9 shows how the pitch affects the droplet size and the generation mode at a flow rate of $5 \mu\text{l}/\text{min}$, which is not the optimal condition for generating the stable droplet. In this experiment, the groove pitch is varied from 80 to $140 \mu\text{m}$. When the oil phase moves from right to left within a cavity, the two-phase interface touches two points: one at the top of the left groove and one at any point on the bottom surface. As the groove pitch increases, contact is delayed and a small main droplet is consequently generated (Fig. 7); this situation corresponds to the case of a slow flow rate. Therefore, a daughter droplet is generated in the right corner of the cavity. For the optimal condition of the droplet generation, the pitch should match with the flow rate. Hence, for the generation of uniform droplets without any daughter droplets, consideration must be given to the synchronization of the contact on the top of the forward groove and that on the bottom of the cavity.

Figure 10 shows the droplet formation time required to generate the type of left-corner spherical droplet shown in Figs. 8 and 9. It also shows the escape time, which refers to the time taken for the droplet to move out of the cavity. As the flow rate is increased, the droplet is generated at a faster rate. We expect this technique to serve as a platform for droplet-based reaction systems, particularly with regard to the monitoring of cell behavior, *in vitro* expression, and possibly even micropolymerase chain reaction chambers.

From the experimental observations, we suppose that there are four key factors of droplet generation: movement of the interface between the oil and aqueous phases into the cavity along the walls, which is related to the viscosity of the oil phase; the velocity of the interface across the cavity; the surface tension between two liquids; and the aspect ratio of the cavity. We attempted to

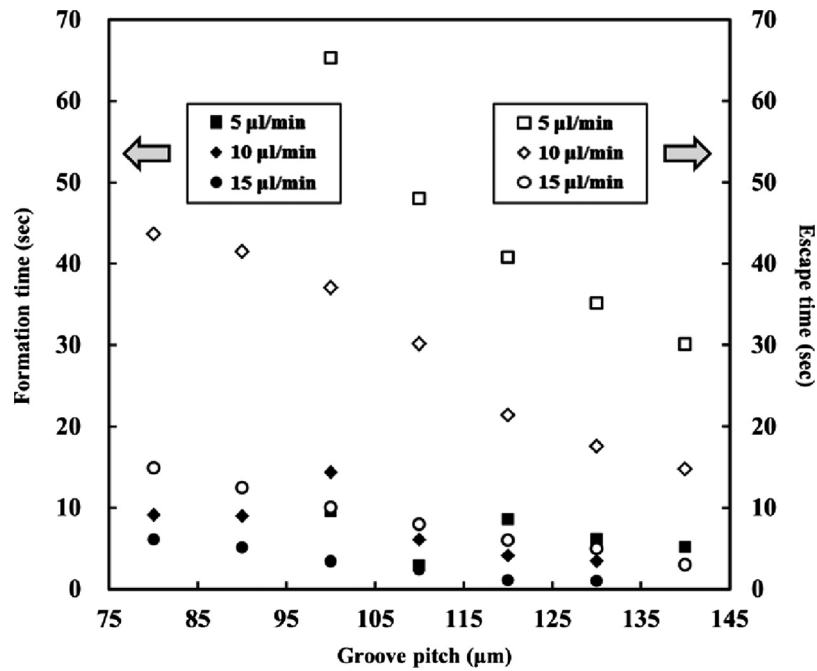


FIG. 10. Effects of flow rate and groove pitch on droplet formation time and escape time.

suggest a dimensionless number for this droplet generation mechanism in a grooved microchannel. The capillary number may be a key factor in determining the interface movement and droplet formation behavior. The capillary number is defined as

$$Ca = \frac{\mu U}{\gamma}, \quad (1)$$

where μ is the viscosity of the continuous phase, U is the velocity of the continuous phase, and γ is the surface tension of the interface. Above a certain capillary number, a droplet break-off occurs.² The critical capillary number depends on system parameters such as the geometry and properties of the fluid. Interestingly, for every viscosity liquid, the single droplets are formed at conditions of 110 μm pitch, 10 $\mu\text{l/min}$ flow rate, and 45 μm height of the groove, which are considered as the optimal conditions.

Figure 11 shows the droplet size according to the capillary number for the silicone oil (20 cP) and water case. If we consider only the optimal condition for generating stably the droplet (pitch of 100 and 110 μm), it notes that the droplet diameter increases according to the capillary number. However, there is a critical capillary number for generating the stable single droplet, which ranges from 0.06 to 0.08. In other cases, the diameter varies randomly and the daughter droplets are generated. One notes that viscosity and surface tension play a role similar to a threshold for the generation of a droplet. Depending on the viscosity of the oil, the contact line on the groove wall should continue moving along the wall and descend to the bottom of the cavity, confining the aqueous phase in the cavity. In addition, the surface tension of the interface is related to the formation of a spherical droplet at the corner in the cavity. Once a droplet can be generated, the optimal conditions for stable droplet generation are directly related to the velocity of the interface and the geometry of the cavity. Of the four key factors noted earlier, the velocity of the interface and the aspect ratio of the cavity also appear to be significant factors for establishing the optimal conditions for generating the droplet.

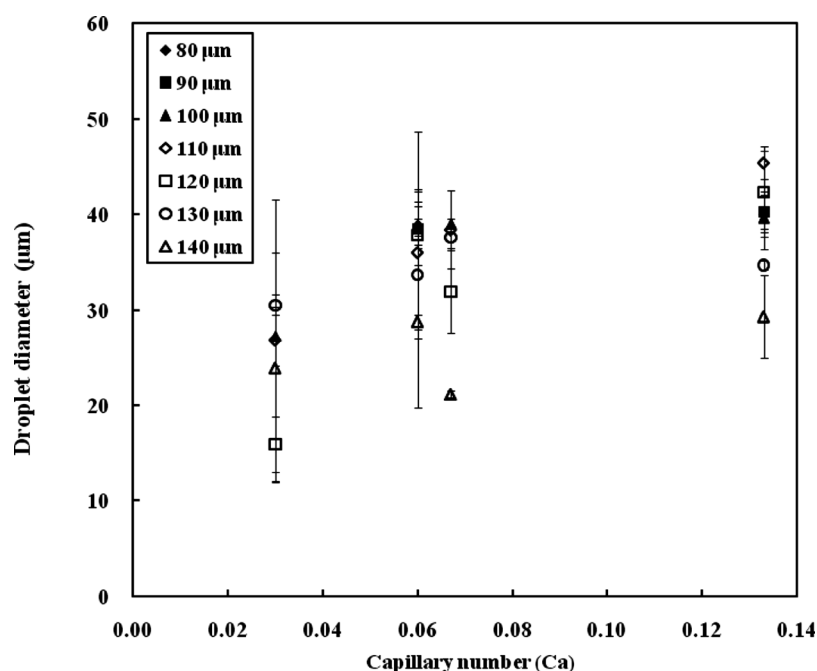


FIG. 11. Effect of the capillary number on the droplet diameter.

IV. CONCLUSION

We have presented a new method of generating droplets stored in microfluidic cavity structures. First we designed and fabricated PDMS microchannels with various grooves on the walls. To investigate wetting and nonwetting transition in relation to the geometrical shape of the grooves, we studied the effects of the flow rate and the pitch between the grooves. We propose three mechanisms for the droplet generation: the contact line on the groove wall should continue moving along the wall and descend to the bottom of the cavity, confining the aqueous phase in the cavity; once the interface between the oil and aqueous phases moves into a cavity, the interface should contact the top of the neighboring groove; and a spherical droplet forms at the corner due to surface tension. The viscosity of the oil phase and the surface tension of the interface determine whether the droplet can be generated. In addition, the velocity of the interface and the aspect ratio of the cavity appear to be significant factors in establishing optimal conditions for generating the largest droplet.

ACKNOWLEDGMENTS

This research was supported by the Basic Science Research Program through the National Research Foundation of Korea, which is funded by the Ministry of Education, Science and Technology (Grant Nos. 2010-0015174 and 2009-0082607). The authors also acknowledge the helpful comments of Dr. DeMello of Imperial College London.

- ¹H. Stone and S. Kim, *AIChE J.* **47**, 1250 (2001).
- ²S. Teh, R. Lin, L. Hung, and A. Lee, *Lab Chip* **8**, 198 (2008).
- ³A. Günther and K. F. Jensen, *Lab Chip* **6**, 1487 (2006).
- ⁴A. Huebner, S. Sharma, M. Srisa-Art, F. Hollfelder, J. Edel, and A. demello, *Lab Chip* **8**, 1244 (2008).
- ⁵H. Song, D. Chen, and R. Ismagilov, *Angew. Chem., Int. Ed.* **45**, 7336 (2006).
- ⁶S. Sugiura, M. Nakajima, S. Iwamoto, and M. Seki, *Langmuir* **17**, 5562 (2001).
- ⁷S. Anna, N. Bontoux, and H. Stone, *Appl. Phys. Lett.* **82**, 364 (2003).
- ⁸T. Kawakatsu, Y. Kikuchi, and M. Nakajima, *J. Am. Oil Chem. Soc.* **74**, 317 (1997).
- ⁹D. R. Link, S. L. Anna, D. A. Weitz, and H. A. Stone, *Phys. Rev. Lett.* **92**, 054503 (2004).
- ¹⁰H. Song and R. Ismagilov, *J. Am. Chem. Soc.* **125**, 14613 (2003).
- ¹¹T. Thorsen, R. Roberts, F. Arnold, and S. Quake, *Phys. Rev. Lett.* **86**, 4163 (2001).

- ¹² S. Cho, S. Fan, H. Moon, and C. Kim, Proc. IEEE Conf. MEMS, 32 (2002) .
- ¹³ S. Cho, H. Moon, and C. Kim, *J. Microelectromech. Syst.* **12**, 70 (2003).
- ¹⁴ Z. Xue-Feng, Y. Rui-Feng, W. Jian-Gang, D. Liang, and L. Li-Tian, *Chin. Phys. Lett.* **21**, 1851 (2004).
- ¹⁵ A. Wixforth, C. Strobl, C. Gauer, A. Toegl, J. Scriba, and Z. v. Guttenberg, *Anal. Bioanal. Chem.* **379**, 982 (2004).
- ¹⁶ D. Beyssen, L. Le Brizoual, O. Elmazria, and P. Alnot, *Sens. Actuators B* **118**, 380 (2006).
- ¹⁷ T. Franke, A. Abate, D. Weitz, and A. Wixforth, *Lab Chip* **9**, 2625 (2009).
- ¹⁸ J. Meacham, C. Ejimofor, S. Kumar, F. Degertekin, and A. Fedorov, *Rev. Sci. Instrum.* **75**, 1347 (2004).
- ¹⁹ J. Meacham, M. Varady, F. Degertekin, and A. Fedorov, *Phys. Fluids* **17**, 100605 (2005).
- ²⁰ D. Byun, J. Kim, H. Ko, and H. Park, *Phys. Fluids* **20**, 113601 (2008).
- ²¹ C. Choi, K. Westin, and K. Breuer, *Phys. Fluids* **15**, 2897 (2003).
- ²² N. Churaev, V. Sobolev, and A. Somov, *J. Colloid Interface Sci.* **97**, 574 (1984).
- ²³ J. Davies, D. Maynes, B. Webb, and B. Woolford, *Phys. Fluids* **18**, 087110 (2006).
- ²⁴ P. Huang and K. Breuer, *Phys. Fluids* **19**, 028104 (2007).
- ²⁵ P. Joseph and P. Tabeling, *Phys. Rev. E* **71**, 035303(R) (2005).
- ²⁶ R. Pit, H. Hervet, and L. Leger, *Phys. Rev. Lett.* **85**, 980 (2000).
- ²⁷ E. Schnell, *J. Appl. Phys.* **27**, 1149 (1956).
- ²⁸ D. Tretheway and C. Meinhart, *Phys. Fluids* **14**, L9 (2002).
- ²⁹ Y. Zhu and S. Granick, *Phys. Rev. Lett.* **87**, 096105 (2001).
- ³⁰ C.-H. Choi and C.-J. Kim, *Phys. Rev. Lett.* **96**, 066001 (2006).
- ³¹ C. Choi, U. Ulmanella, J. Kim, C. Ho, and C. Kim, *Phys. Fluids* **18**, 087105 (2006).
- ³² J. Tyrrell and P. Attard, *Phys. Rev. Lett.* **87**, 176104 (2001).
- ³³ R. Wenzel, *Ind. Eng. Chem.* **28**, 988 (1936).
- ³⁴ A. Cassie and S. Baxter, *Trans. Faraday Soc.* **40**, 546 (1944).
- ³⁵ L. Barbieri, E. Wagner, and P. Hoffmann, *Langmuir* **23**, 1723 (2007).
- ³⁶ Y. Chen, B. He, J. Lee, and N. Patankar, *J. Colloid Interface Sci.* **281**, 458 (2005).
- ³⁷ A. Lafuma and D. Quere, *Nature Mater.* **2**, 457 (2003).
- ³⁸ N. Patankar, *Langmuir* **20**, 7097 (2004).
- ³⁹ S. Maheshwari, L. Zhang, Y. Zhu, and H.-C. Chang, *Phys. Rev. Lett.* **100**, 044503 (2008).
- ⁴⁰ G. Parikesit, E. Vrouwe, M. Blom, and J. Westerweel, *Biomicrofluidics* **4**, 044103 (2010).
- ⁴¹ H. Ma, L. Jiang, W. Shi, J. Qin, and B. Lin, *Biomicrofluidics* **3**, 044114 (2009).
- ⁴² L. Yeo and J. Friend, *Biomicrofluidics* **3**, 012002 (2009).